CMB probes for cosmology and particle physics

Martin BUCHER

Laboratoire APC (Astroparticles & Cosmologie)

Université Paris 7 (Denis-Diderot)/CNRS

15 May 2017

Russian National Research Nuclear University MEPHI

Moscow, Russian Federation

Lecture 12 of "Introduction to Cosmoparticle Physics" Course

Basic reference :

Physics of the cosmic microwave background anisotropy

Martin Bucher (Laboratoire APC, Université Paris 7/CNRS, Paris, France and School of Mathematics, Statistics and Computer Science, University of KwaZulu-Natal, Durban, South Africa)

(Submitted on 18 Jan 2015)

Observations of the cosmic microwave background (CMB), especially of its frequency spectrum and its anisotropies, both in temperature and in polarization, have played a key role in the development of modern cosmology and our understanding of the very early universe. We review the underlying physics of the CMB and how the primordial temperature and polarization anisotropies were imprinted. Possibilities for distinguishing competing cosmological models are emphasized. The current status of CMB experiments and experimental techniques with an emphasis toward future observations, particularly in polarization, is reviewed. The physics of foreground emissions, especially of polarized dust, is discussed in detail, since this area is likely to become crucial for measurements of the B modes of the CMB polarization at ever greater sensitivity.
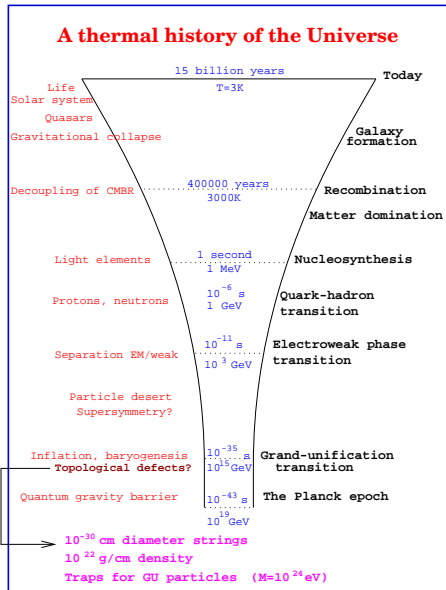
Thermal history of the Universe

A thermal history of the Universe

CMB — What are we looking at today?

We are here today observing the CMB

$t_0 =$

t (time)

Universe transparent

Last scattering surface

Universe Opaque

Putative big bang

$t_{z=1100} \approx 3 \times 10^5 \, yrs$

$t = 0$

$x_e \approx 1$ Photons diffuse (random walk)

X (space)

$$ds^2 = -dt^2 + a^2(t)\left[dx^2 + dy^2 + dz^2\right]$$

$$a(t) \equiv \text{scale factor}$$

Scale factors

$a(t) \sim t^{1/2}$ radiation-dominated universe   (R.D.)

$a(t) \sim t^{2/3}$ matter-dominated universe   (M.D.)

$a(t) \sim e^{Ht}$ vacuum-energy (cosmological constant)

           dominated universe   (V.D.)

        [aka 'de Sitter space']

$a(\eta) \sim \eta$

$\boxed{\eta = \int \dfrac{dt}{a(t)}}$

$a(\eta) \sim \eta^2$

$ds^2 = a^2(\eta)\left[-d\eta^2 + d\underset{\sim}{x}^2\right]$

$= -dt^2 + a^2(t)\, d\underset{\sim}{x}^2$

$a(\eta) \sim \dfrac{-1}{\eta}$

$t \equiv$ proper (clock) time

$\eta \equiv$ conformal time
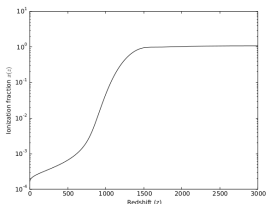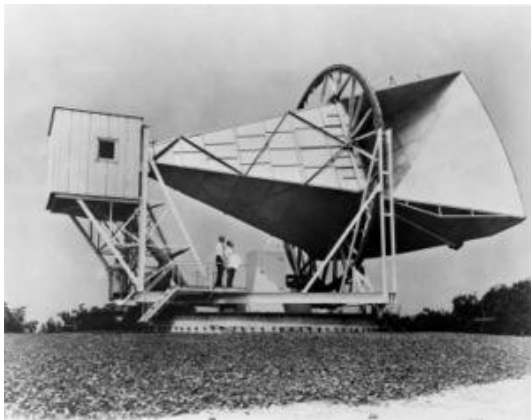
Here $\boxed{-\infty < \eta < 0.}$

Figure 11: **Ionization fraction as function of redshift with effect of late-time ionizing radiation ignored.** Calculated using the code *Cosmo Rec* by Jens Chluba (for details see Ref. [213]).

Saha equlibrium (approximate description)

$$\frac{x_e{}^2}{(1 - x_e)} = \frac{n_Q}{n_B} \exp\left[-\frac{E_I}{i k_B T}\right]$$

where $E_I = 13.4$ eV and

$$n_Q = \left(\frac{2\pi m_e K_B T}{\hbar^2}\right)^{3/2}.$$

We may rewrite

$$
\begin{aligned}
\frac{n_Q}{n} &= \frac{O(1)}{n_B} \left(\frac{m_e c^2}{k_B T}\right)^{3/2} \left(\frac{k_B T}{\hbar c}\right)^3 \\
&= O(1) \left(\frac{m_e c^2}{k_B T}\right)^{3/2} \left(\frac{n_\gamma}{n_B}\right).
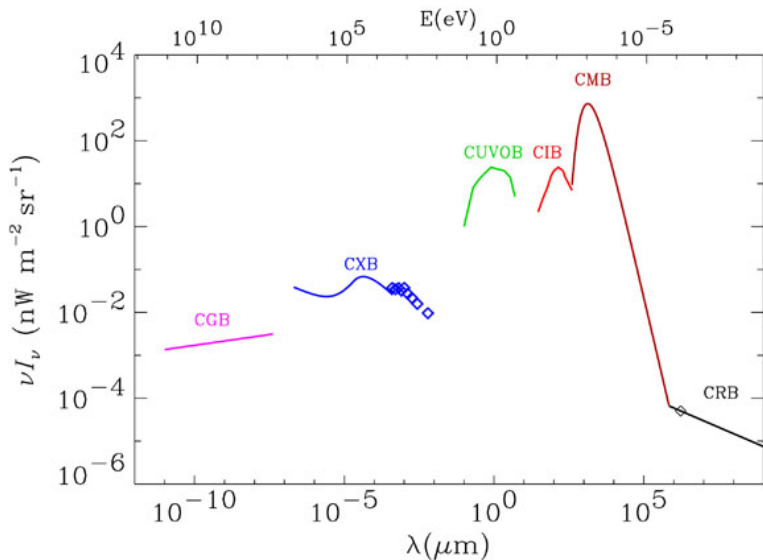\end{aligned}
$$

Summary so far

- The microwave background that we see today is a nearly perfect blackbody having a nearly isotropic temperature of 2.75 K.

- Over the almost all of the 13.4×10^{10} years of cosmic history—that is, over 99.997% of this history, $\approx 94\%$ of the microwave photons propagated to us without ever being rescattered.

- Only during approximately the first 380,000 years since the putative Big Bang was scattering appreciable, before the universe cooled down, allowing the primordial plasma to transform into neutral hydrogen and helium.

- The agreement of the CMB energy spectrum with a perfect blackbody provides strong confirmation of the hot big bang model.

- The temperature fluctuations (at the level of approximately 1 part in 10^5) provide a sensitive probe of the initial conditions of our universe. Roughly speaking, observing the CMB provides a snapshot of the state the universe on a sphere of radius 45 Billion light years, almost all the way back to the putative Big Bang, at an epoch when the cosmological perturbations were small and well described by linear theory. [Question : Why does this radius exceed the age of the universe ?]

Discovery of the cosmic microwave ackground

1963 Penzias and Wilson (Bell Labs) observed a background of microwaves having a thermal spectrum with $T = 2.753 K$. This temperature is (almost) the same no matter what the direction in the sky.
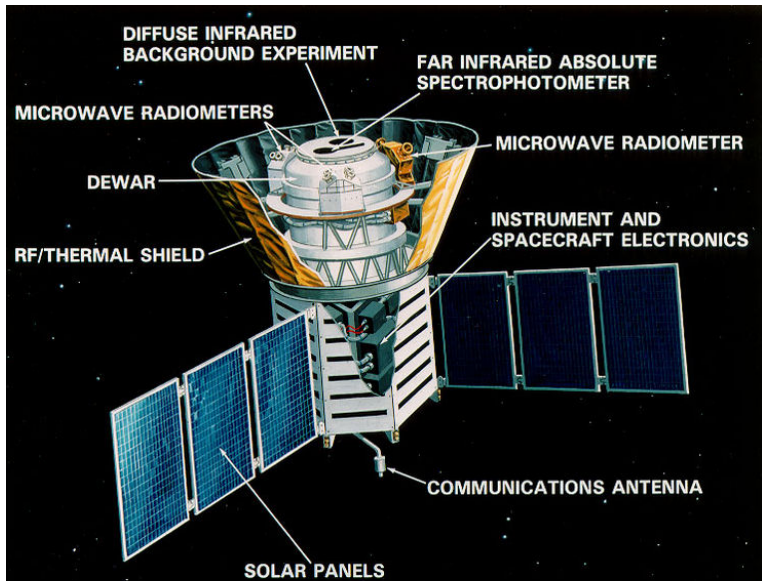
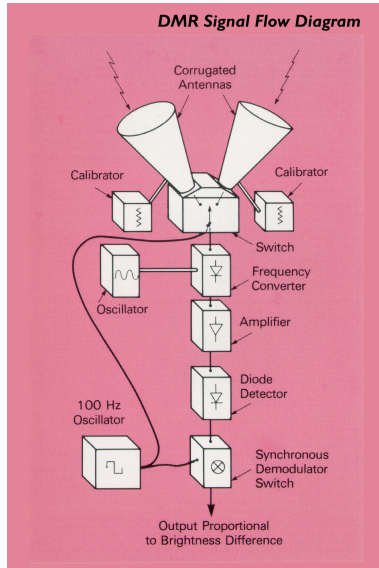# Electromagnetic radiation energy content of Universe

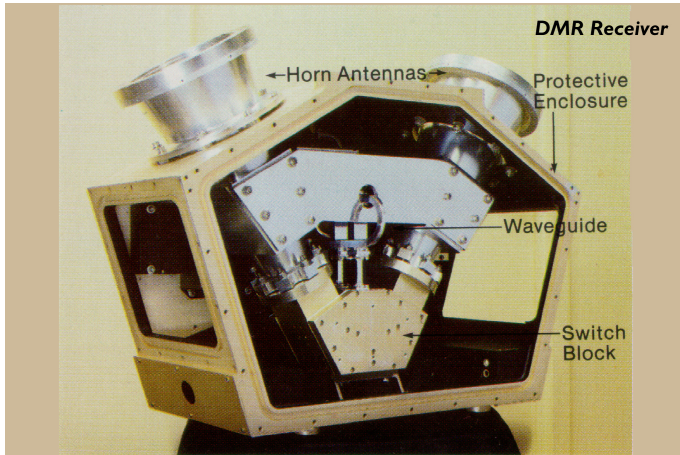## COBE DMR (Differential Microwave Radiometer) Instrument block diagram

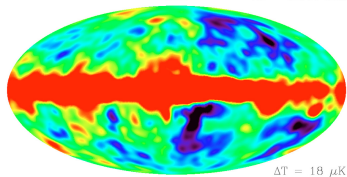# COBE DMR (Differential Microwave Radiomete) Instrument block diagram

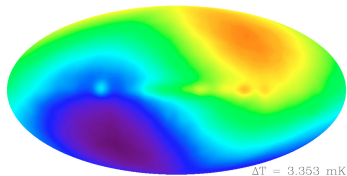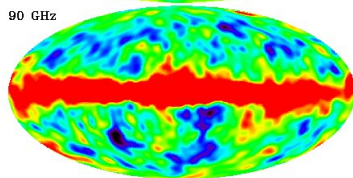# DMR instrument

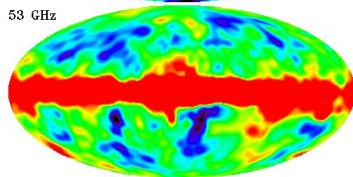# Raw COBE CMB maps with successive subtractions

DMR 53 GHz Maps

T = 2.728 K

ΔT = 3.353 mK

ΔT = 18 μK

COBE DMR (Differential Microwave Radiometer) frequency maps

31.5 GHz

53 GHz

90 GHz

−100 μK   +100 μK

How best to interpret the maps ?

Two-point function of an isotropic Gaussian random process.

$$\delta T(\hat{n}) = \sum_{\ell=0}^{\infty} \sum_{m=-\ell}^{+\ell} a_{\ell m} \, Y_{lm}(\hat{n})$$

$$\langle a_{\ell m}^{*} a_{\ell' m'} \rangle = \delta_{\ell \ell'} \delta_{mm'} c_{\ell}$$

$$c_{\ell}^{(sky)} = \frac{1}{(2\ell + 1)} \sum_{m=-\ell}^{+\ell} \left| a_{\ell m} \right|^2$$

Cosmic variance — we have only one sky to observe

$c_\ell^{(sky)}$ obeys a χ^2 distribution with $(2\ell + 1)$ degrees of freedom.

Probability of CMB temperature sky map given a theory

$$P\left(\{a_{\ell m}\}\,\bigg|\,\left\{c_\ell^{(th)}\right\}\right) = \prod_{\ell=0}^{\infty} \prod_{m=-\ell}^{+\ell} \frac{1}{\sqrt{2\pi c_\ell^{(th)}}} \exp\left[-\frac{1}{2}\left|a_{\ell m}\right|^2\right]$$

Or we can express the result in terms of a log likelihood

$$\ln P\left(\left\{c_\ell^{(obs)}\right\}\,\bigg|\,\left\{c_\ell^{(th)}\right\}\right) = \sum_{\ell=0}^{\infty}(2\ell+1)\left(\frac{c_{obs}}{c_{th}} - 1 + \ln\left(\frac{c_{obs}}{c_{th}}\right)\right) + (\mathrm{constant})$$

Error due to cosmic variance :

$$\left(\frac{\delta c_\ell}{c_\ell}\right)_{obs} = \sqrt{\frac{2}{2\ell+1}}$$
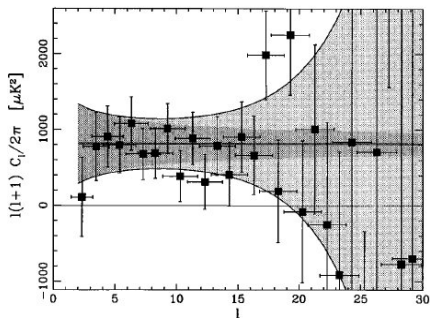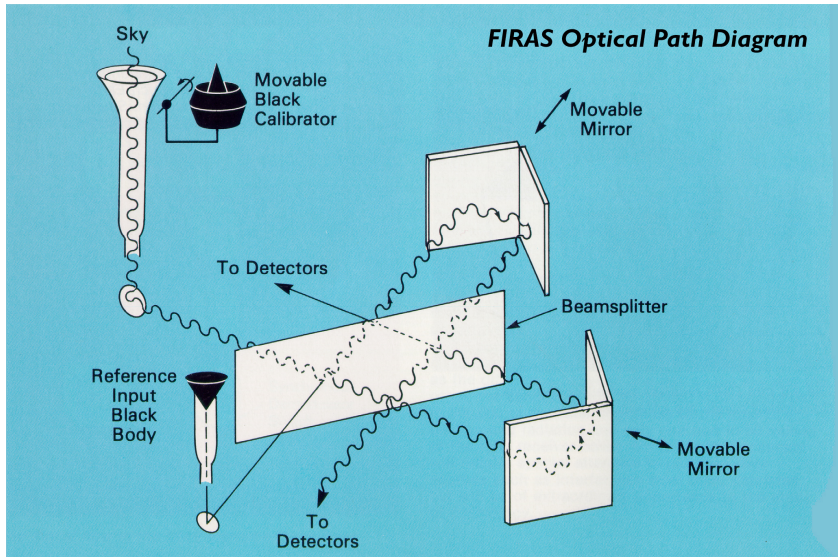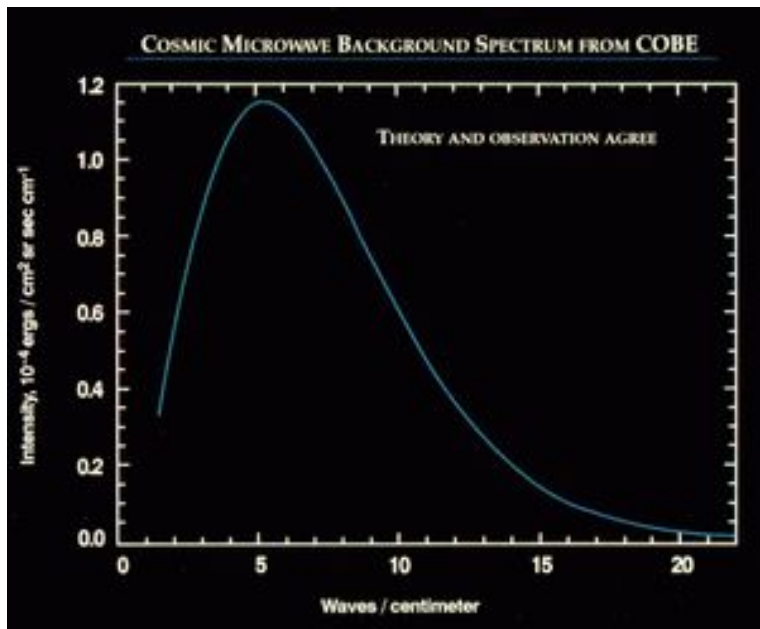
COBE DMR angular power spectrum

FIG. 1.—Power spectrum observed by *COBE*. The observed multipoles $D_\ell = \ell(\ell + 1)C_\ell$ are plotted with 1 σ error bars. The vertical error bars include both pixel noise and cosmic variance, and the horizontal bars show the width of the window functions used. If the true power spectrum is given by $n = 1$ and $Q_{rms, ps} = 18.4 \ \mu K$ (*heavy horizontal line*), then the shaded region gives the 1 σ error bars and the dark-shaded region shows the contribution from cosmic variance.
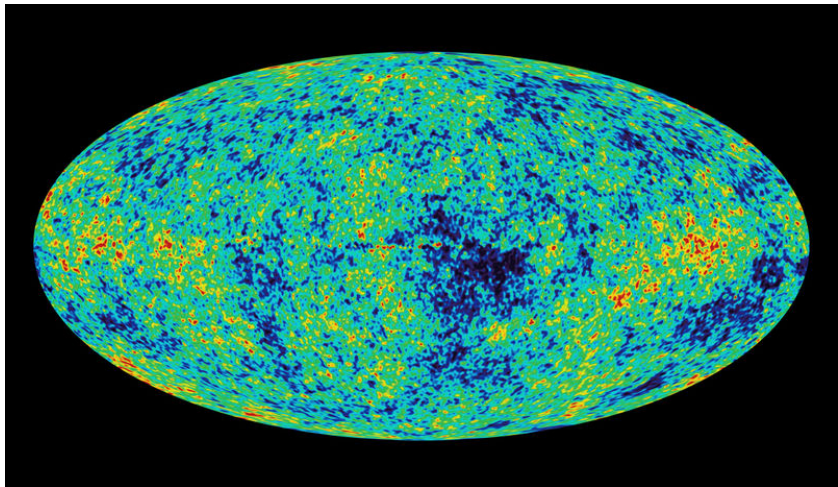
from Tegmark (1996)

FIRAS instrument concept

FIRAS Optical Path Diagram

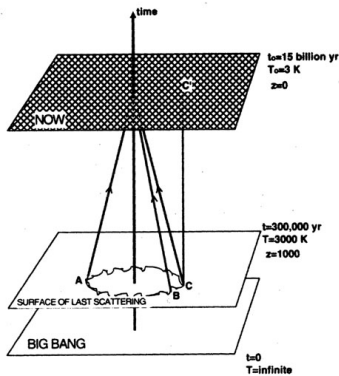# FIRAS determination of frequency spectrum

Preview of WMAP

Theory – origin of the CMB anisotropy

Sachs-Wolfe formula

$$\frac{\delta T}{T}(\hat{\mathbf{n}}) = \left[\frac{1}{4}\delta_\gamma + \mathbf{v}_\gamma \cdot \mathbf{n} + \Phi i\right]_i^f + 2\int_i^f d\eta \frac{\partial \Phi'}{\partial \eta}(\eta, \hat{\mathbf{n}}(\eta_0 - \eta))$$

$\Phi \equiv$ Newtonian gravitational potential (dimensionless)
δ_γ and $\mathbf{v}_\gamma$ describe the fractional density contrast and peculiar 3-velocity of of the photon component.

This treatment is somewhat naive because it assumes that the surface of last scatter is infinitely thin.
In reality the surface of last scatter has a width the smears the anisotropies on small scales.
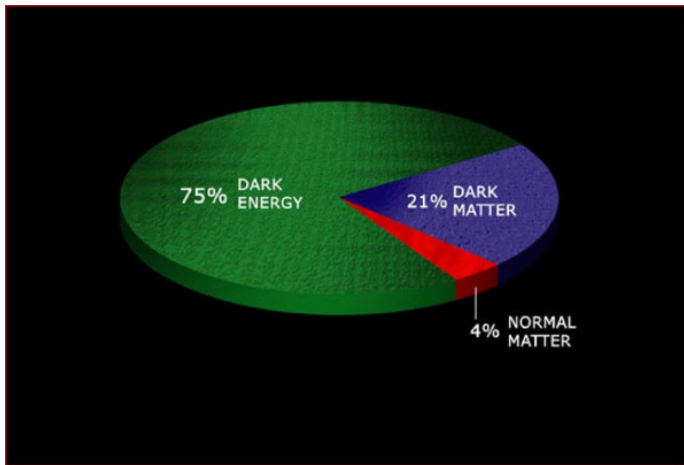
CMB anisotropies - toward a more careful treatment

A exact treatment must consider keep track of both photon polarizations and the entire angular distribution function, which requires in principle an infinite number of variables. Here are the photon equations :

$$\dot{\delta}_\gamma = -\frac{4}{3}\theta_\gamma + 4\dot{\phi},$$

$$\dot{\theta}_\gamma = k^2\left(\frac{1}{4}\delta_\gamma - \sigma_\gamma\right) + k^2\psi + an_e\sigma_T(\theta_b - \theta_\gamma),$$

$$\dot{F}_{\gamma 2} = 2\dot{\sigma}_\gamma = \frac{8}{15}\theta_\gamma - \frac{3}{5}kF_{\gamma 3} - \frac{9}{5}an_e\sigma_T\sigma_\gamma + \frac{1}{10}an_e\sigma_T\left(G_{\gamma 0} + G_{\gamma 2}\right),$$

$$\dot{F}_{\gamma l} = \frac{k}{2l+1}\left[lF_{\gamma(l-1)} - (l+1)F_{\gamma(l+1)}\right] - an_e\sigma_T F_{\gamma l}, \quad l \geq 3$$

$$\dot{G}_{\gamma l} = \frac{k}{2l+1}\left[lG_{\gamma(l-1)} - (l+1)G_{\gamma(l+1)}\right] + an_e\sigma_T\left[-G_{\gamma l} + \frac{1}{2}\left(F_{\gamma 2} + G_{\gamma 0} + G_{\gamma 2}\right)\left(\delta_{l0} + \frac{\delta_{l2}}{5}\right)\right]$$

These are not very enlightening and accurate calculations are carried out using codes like CAMB. Nevertheless simplified treatments are essential for gaining intuition and understanding the output of the numerical results.

Components of the present mean energy density of the universe

Ingredients for modelling CMB multipole spectrum

Component contributing to the stress-energy-momentum tensor :

- Baryons (protons, nuclei, and accompanying electrons) Strong coupling to photons provide springiness. Pressure prevents gravitational clustering

- Neutrinos (collisionless, do not scatter)

- Photons. Relativistic. Initially tightly coupled to baryons, and cannot go anywhere because of Thomson scattering. After plasma disappears due to recombination to neutral atomic Hydrogen and Helium, travel along geodesics.

- Dark matter (collisionless non-relativistic component, or cold dust) Can cluster before baryons because does not scatter with photons.
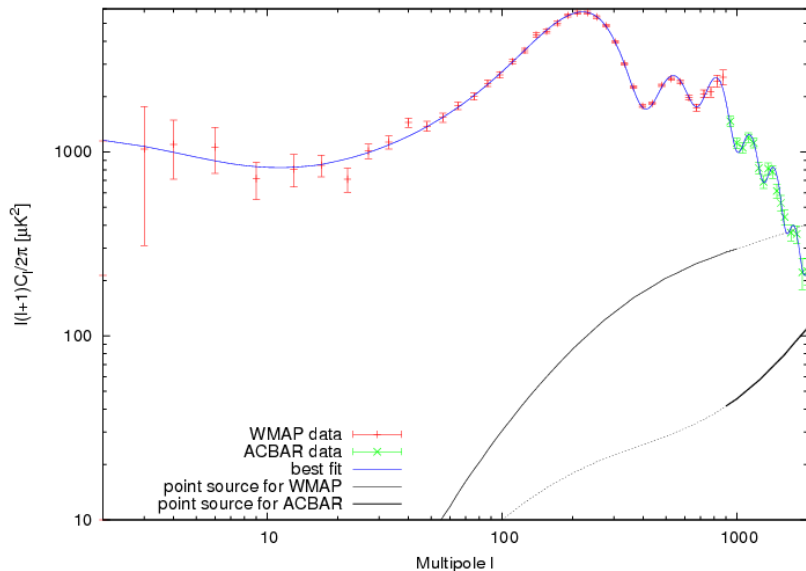
- Dark energy or cosmological constant

Primordial power spectrum :
$P(k) = A_S(k/k*)^{n_S}$ where k^* is the pivot scale.

Parameters :
H_0, $\omega_b = h^2\Omega_b$, $\omega_{cdm} = h^2\Omega_{cdm}$, Ω_Λ, w (optional), n_s, τ_{reion}

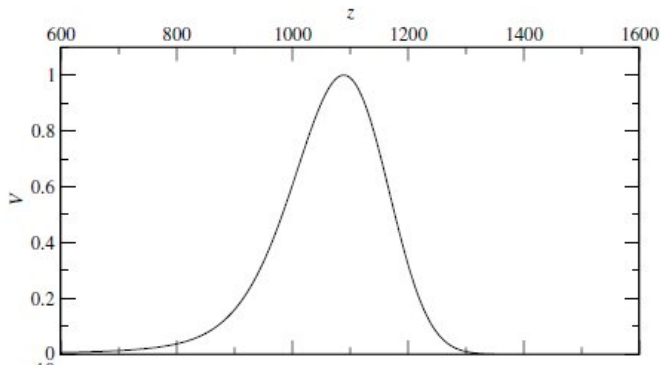# Simple model fited to WMAP and ACBAR

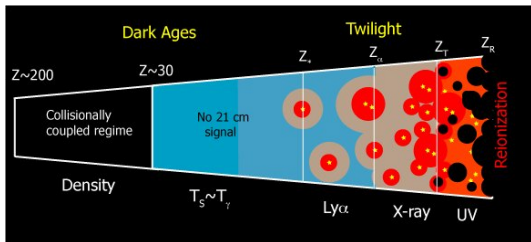WMAP Cosmological Parameters

Model: lcdm+sz+lens

Data: wmap5

$10^2\Omega_b h^2$	2.273 ± 0.062	$1 - n_s$	$0.037^{+0.015}_{-0.014}$
$1 - n_s$	$0.0081 < 1 - n_s < 0.0647$ (95% CL)	$A_{\mathrm{BAO}}(z = 0.35)$	0.457 ± 0.022
C_{220}	5756 ± 42	$d_A(z_{\mathrm{eq}})$	14279^{+186}_{-189} Mpc
$d_A(z_*)$	14115^{+188}_{-191} Mpc	$\Delta^2_{\mathcal{R}}$	$(2.41 \pm 0.11) \times 10^{-9}$
h	$0.719^{+0.026}_{-0.027}$	H_0	$71.9^{+2.6}_{-2.7}$ km/s/Mpc
k_{eq}	0.00968 ± 0.00046	ℓ_{eq}	136.6 ± 4.8
ℓ_*	$302.08^{+0.83}_{-0.84}$	n_s	$0.963^{+0.014}_{-0.015}$
Ω_b	0.0441 ± 0.0030	$\Omega_b h^2$	0.02273 ± 0.00062
Ω_c	0.214 ± 0.027	$\Omega_c h^2$	0.1099 ± 0.0062
Ω_Λ	0.742 ± 0.030	Ω_m	0.258 ± 0.030
$\Omega_m h^2$	0.1326 ± 0.0063	$r_{\mathrm{hor}}(z_{\mathrm{dec}})$	286.0 ± 3.4 Mpc
$r_s(z_d)$	153.3 ± 2.0 Mpc	$r_s(z_d)/D_v(z = 0.2)$	0.1946 ± 0.0079
$r_s(z_d)/D_v(z = 0.35)$	0.1165 ± 0.0042	$r_s(z_*)$	146.8 ± 1.8 Mpc
R	1.713 ± 0.020	σ_8	0.796 ± 0.036
A_{SZ}	$1.04^{+0.96}_{-0.69}$	t_0	13.69 ± 0.13 Gyr
τ	0.087 ± 0.017	θ_*	0.010400 ± 0.000029
θ_*	0.5959 ± 0.0017 °	t_*	380081^{+5843}_{-5841} yr
z_{dec}	1087.9 ± 1.2	z_d	1020.5 ± 1.6
z_{eq}	3176^{+151}_{-150}	z_{reion}	11.0 ± 1.4
z_*	1090.51 ± 0.95		

Visibility function

From what redshift are the CMB photons coming (i.e., redshift of last scatter) ?
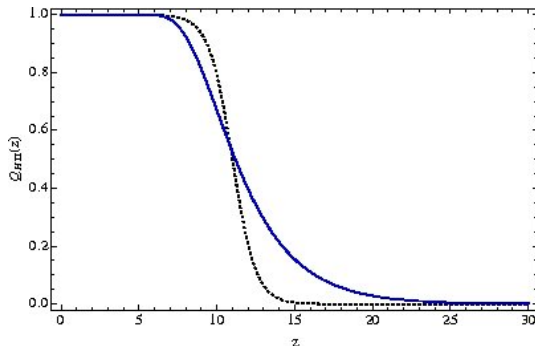
Reionization of the neutral hydrogen at intermediate redshift
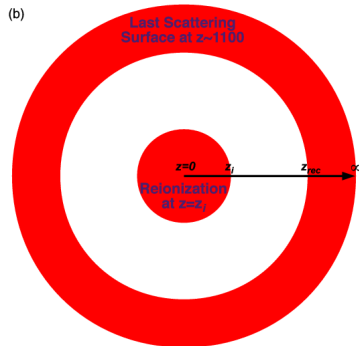

The first stars and quasars generate ionizing UV photons transforming the neutral hydrogen into free protons, He4 nuclei, and electrons.
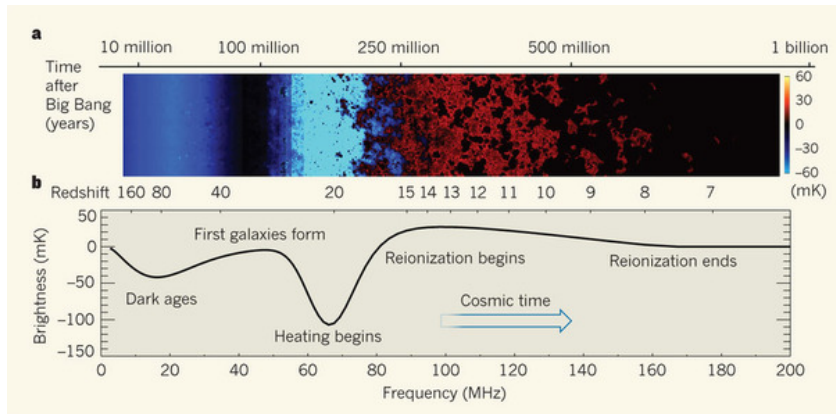
Possible reionization histories

We do not know what the precise average reionization history is. It is described by a function $\tau(z)$. But the CMB has little sensitivity, and often τ is modelled under the approximation of instantaneous reionization.
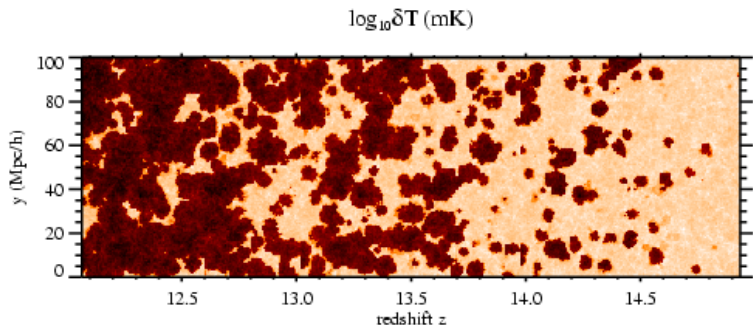
Effect of reionization on the CMB anisotropies

A CMB photon has a chance $(1 - \exp(\tau))$ of being unscattered. This component maintains its original anistropies from the surface of last scatter. For fraction $\exp(\tau)$ of the photons that are rescattered recently, all the CMB anisotropy is erased except for the anisotropy on the very largest scales

Inhomgeneous reionization

Reionization simulations (for future 21cm observations)

$\log_{10} \delta \mathbf{T}$ (mK)

The following animations of the shape of the CMB spectrum as a function of the various cosmological parameters are courtesy of Wayne Hu, University of Chicago

background.uchicago.edu/~whu/

Dependence of C_{TT} on Ω_b animation

Dependence of C_{TT} on Ω_k animation

Dependence of C_{TT} on $\omega_b = h^2\Omega_b$ animation

Dependence of C_{TT} on $\omega_{cdm} = h^2 \Omega_{cdm}$ Animation

Dependence of C_{TT} on Ω_{cdm} animation
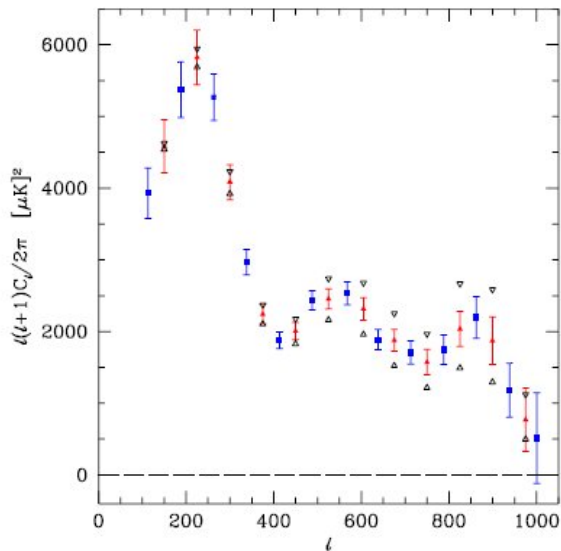
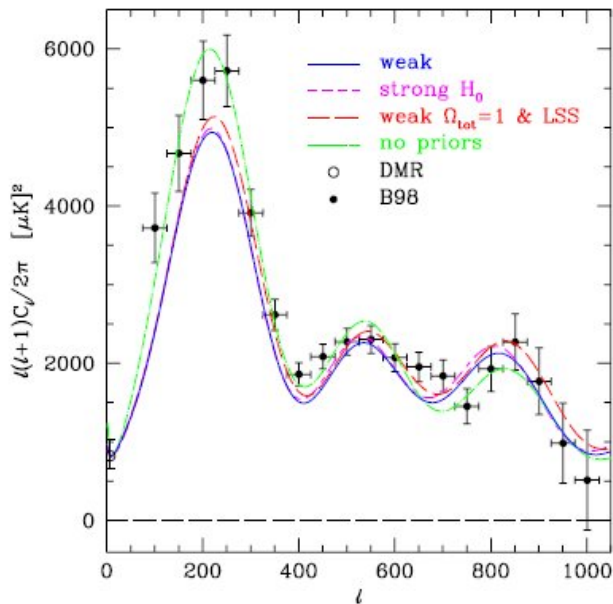# Dependence of C_{TT} on τ animation

Boomerang instrument

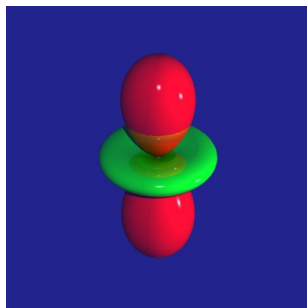# Boomerang baloon

Boomerang mutipole spectrum (no theory)

Boomerang mutipole spectrum (with theory)

CMB polarization
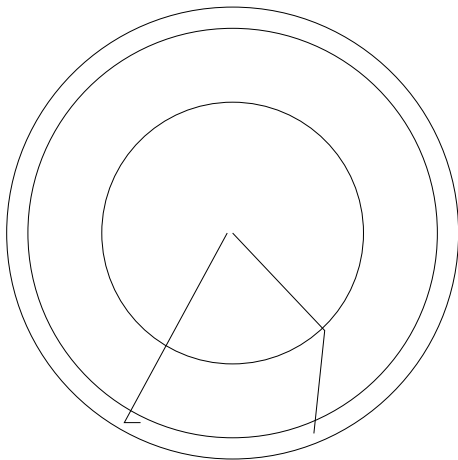
Polarized Thomson scattering ($\gamma + e^- \to \gamma + e^-$) is anisotropic.

$$\sigma_{Thomson} \propto (\epsilon_{in} \cdot \epsilon_{out})^2$$
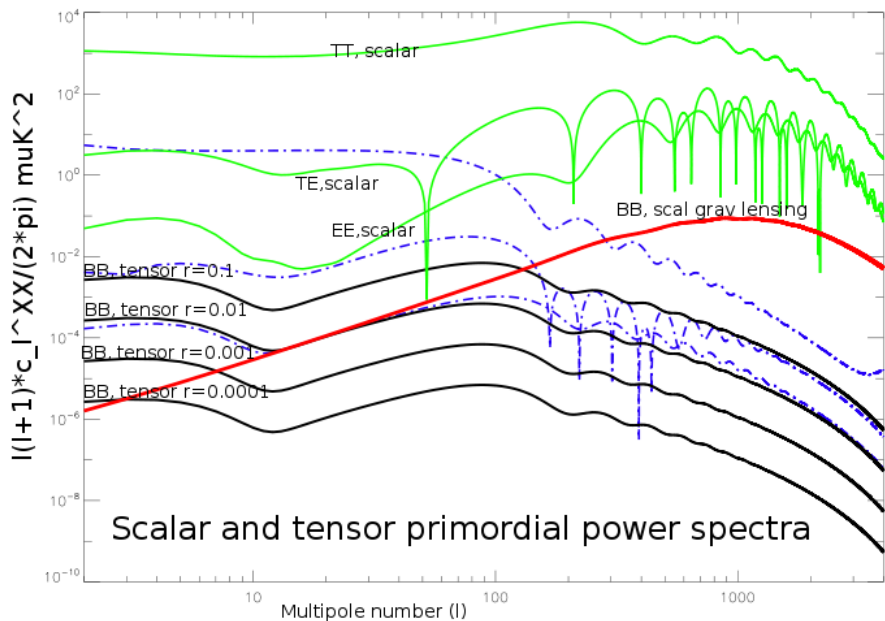

When we look at the polarization of the CMB today, we measure (roughly speaking) the CMB quadrupole seen by the electron at last scattering, which may be due to (1) intrinsic temperature fluctuations, (2) gravitational redshift, or (3) Doppler shift from shear of the velocity field.
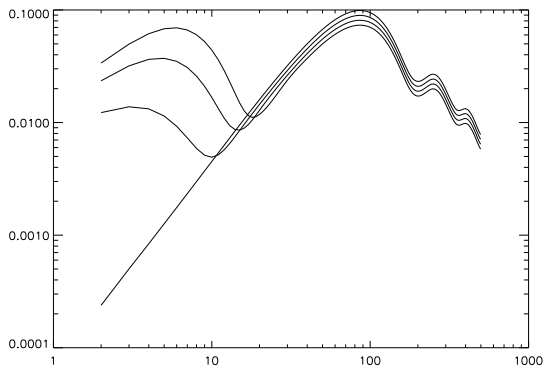
Finite width of surface of last scatter gives rise to polarization of the CMB

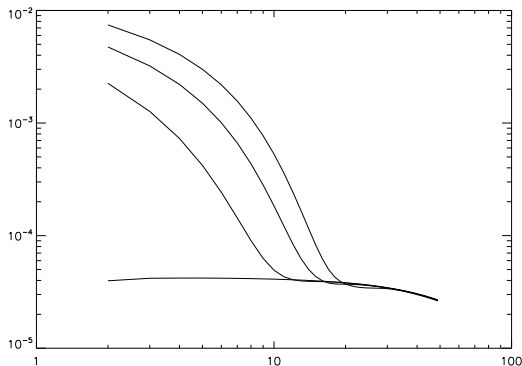Roughly speaking the polarization is a measure of the quadrupole as seen by the electron of last scatter.

Scalar and tensor primordial power spectra
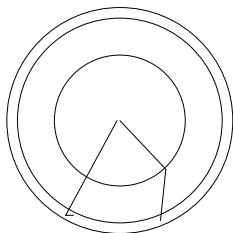
The Reionization Bump (I)

$\tau = 0.0, 0.5, 0.10, 0.15$ (bottom $\rightarrow$ top)

The Reionization Bump (II)

Amplification of the B mode signal relative to the non reionized case by a factor of about 50,100, and 150 at $\tau = 0.05$, $\tau = 0.10$, and $\tau = 0.15$, respectively.

The Reionization Bump (III)

It turns out that

$$P \propto (1 - \tau)d^2_{lastscatter}\frac{\partial^2 T}{\partial x^2}$$

is small compared to

$$P \propto \tau d^2_{reion}\frac{\partial^2 T}{\partial x^2}$$

even when τ is small.

Sources of the CMB polarization (known and possible)

- E-mode polarization
  - Scalar modes (presumably from inflation) (already seen)
  - Tensor modes (presumably from inflation) (not yet seen)
  - Cosmic strings, more generally any non-linear late time source (speculative)
  - Polarized foreground emission (galactic dust, synchrotron, IR galaxies, spinning dust,.....) (seen but not well characterized)
- B mode polarization
  - Tensor modes (presumably from inflation) (not yet seen)
  - Gravitational lensing ($E + \Phi \rightarrow B$) (not yet seen, but certainly there and well understood and calculable)
  - Polarized foreground emission (galactic dust, synchrotron, IR galaxies, spinning dust,.....) (seen but not well characterized)
  - Cosmic strings, more generally any non-linear late time source (speculative)
  - Magnetic fields at recombination ($E \rightarrow B$ Faraday rotation) (speculative)
  - Something else (?)

E and B Mode Polarization

E mode   B mode

$$\mathbf{Y}_{\ell m,ab}^{(E)} = \sqrt{\frac{2}{(\ell-1)\ell(\ell+1)(\ell+2)}} \left[\nabla_a\nabla_b - \frac{1}{2}\delta_{ab}\right] Y_{\ell m}(\hat{\Omega})$$

$$\mathbf{Y}_{\ell m,ab}^{(B)} = \sqrt{\frac{2}{(\ell-1)\ell(\ell+1)(\ell+2)}} \frac{1}{2} \left[\epsilon_{ac}\nabla_c\nabla_b + \nabla_a\epsilon_{bc}\nabla_c\right] Y_{\ell m}(\hat{\Omega})$$

Projection of "scalars," "vectors" and "tensors" onto the celestial sphere

Under projection onto the celestial sphere :

$$(scalar)_3 \rightarrow (scalar)_2,$$

$$(vector)_3 \rightarrow (scalar)_2 + (vector)_2,$$

$$(tensor)_3 \rightarrow (scalar)_2 + (vector)_2.$$

There is no $(tensor)_2$ component. The E mode polarization is scalar ; the B mode is vector.
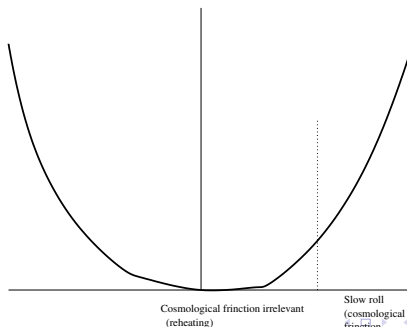
It follows that at linear order the scalar modes cannot generate any B mode polarization.

Note crucial role of linearity assumption.

Single-Field Inflation

In the beginning there was a scalar field that dominated the universe. Everything came from this scalar field and there was nothing without the scalar field. The quantum fluctuations of this field (that is, those of the vacuum) generated small fluctuations that advanced or retarded the instant of re-heating. These were the seeds of the large-scale structure.

$$\ddot{\phi} + 3H\dot{\phi} = -V_{,\phi}$$

Cosmological frinction irrelevant (reheating)

Slow roll (cosmological frinction

Perturbations generated during inflation

$$\boxed{\hbar = c = 1, M_{pl}^{-2}} \qquad \delta\phi \approx H \qquad \frac{\delta\rho}{\rho} \approx H \cdot \delta t, \quad \delta t \approx \frac{\delta\phi}{\dot\phi}$$

$$H\dot\phi \approx V_{,\phi}, \quad \dot\phi \approx V_{,\phi}/H, \quad H^2 \approx \frac{1}{M_{pl}^2} V, \frac{\delta\rho}{\rho} \approx \frac{V^{3/2}[\phi(k)]}{M_{pl}^3 \, V_{,\phi}}$$

Scalar perturbations :
$$\boxed{\mathcal{P}_S^{1/2}(k) \approx O(1) \cdot \frac{V^{3/2}[\phi(k)]}{M_{pl}^3 \, V_{,\phi}[\phi(k)]}} \cdot$$
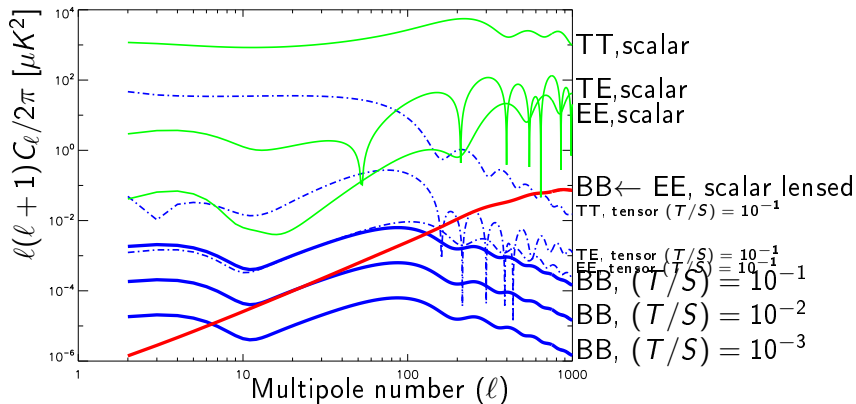
Tensor perturbations :
$$\boxed{\mathcal{P}_T^{1/2}(k) \approx O(1) \cdot \frac{H}{M_{pl}} \approx O(1) \cdot \frac{V^{1/2}}{M_{pl}^2}}$$

$\phi(k) \equiv$ value of ϕ at horizon crossing of the mode k

Reconstruction of the inflationary potential : the tensors measure the height of the potential, the scalars the slope.

Inflationary Prediction for Scalar & Tensor Anisotropies

Lensing of the E mode into the B mode — ($E^{scalar} + \Phi \rightarrow B^{scalar}$)

(Flat sky approximation : $(\ell m) \rightarrow \boldsymbol{\ell}, \quad \boldsymbol{\theta}, \boldsymbol{\ell} \in \mathcal{R}^2$.)

$$\delta\boldsymbol{\theta} = (\boldsymbol{\nabla}\Phi), \qquad \delta T(\boldsymbol{\theta}) = (\boldsymbol{\nabla}\Phi) \cdot (\boldsymbol{\nabla} T).$$

$$\delta T(\boldsymbol{\ell}_F) = \int \frac{d^2\boldsymbol{\ell}_L}{(2\pi)^2} \; (-\boldsymbol{\ell}_L) \cdot (\boldsymbol{\ell}_F - \boldsymbol{\ell}_L) \; \Phi(\boldsymbol{\ell}_L) \; T(\boldsymbol{\ell}_F - \boldsymbol{\ell}_L).$$

$$\langle T(\boldsymbol{\ell}) \; T(\boldsymbol{\ell}') \rangle = (2\pi)^2 \; \delta^2(\boldsymbol{\ell} + \boldsymbol{\ell}') \; C^{TT}(\ell)$$

$$C^{TT}(\boldsymbol{\ell}_F) = \int \frac{d^2\boldsymbol{\ell}_L}{(2\pi)^2} \; [\boldsymbol{\ell}_L \cdot (\boldsymbol{\ell}_F - \boldsymbol{\ell}_L)]^2 \; C^{\Phi\Phi}(\boldsymbol{\ell}_L) \; C^{TT}(\boldsymbol{\ell}_I = |\boldsymbol{\ell}_F - \boldsymbol{\ell}_L|)$$

$$C^{BB}(\boldsymbol{\ell}_B) = \int \frac{d^2\boldsymbol{\ell}_L}{(2\pi)^2} \; [\boldsymbol{\ell}_L \cdot (\boldsymbol{\ell}_F - \boldsymbol{\ell}_L)]^2 \; \sin^2[2\Theta(\boldsymbol{\ell}_B, \boldsymbol{\ell}_E)] C^{\Phi\Phi}(\boldsymbol{\ell}_L) \; C^{EE}(\boldsymbol{\ell}_E = |\boldsymbol{\ell}_B - \boldsymbol{\ell}_L|)$$
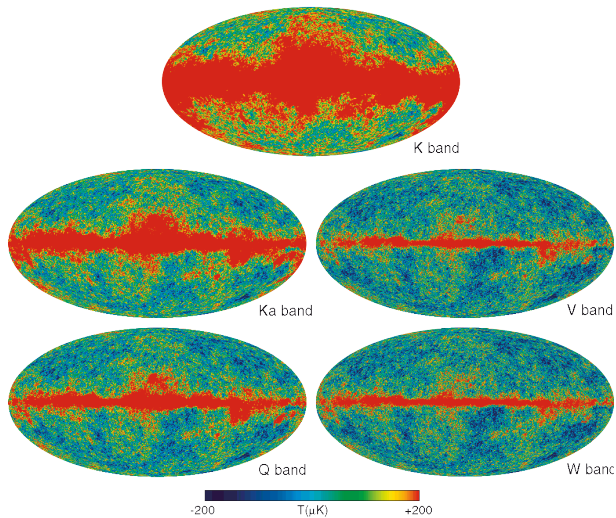
The detection of B modes

The B mode is that component that cannot be represented as a double gradient on the celestial sphere. In the linear approximation there is no B mode component arising from scalar degrees of freedom. The presence of the B mode would unambiguously signal the presence of primordial gravitational waves.
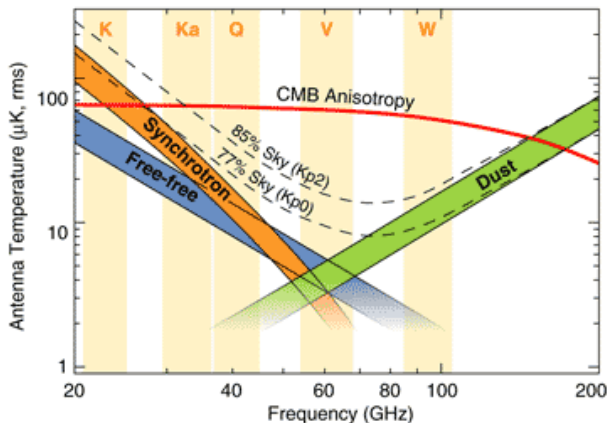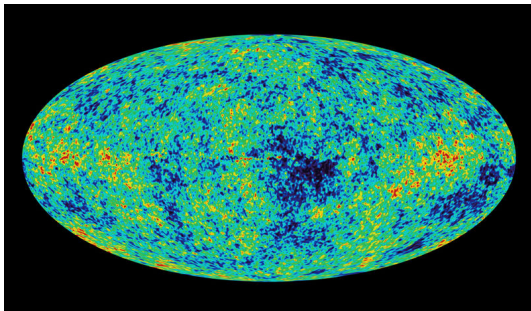
WMAP Temperature Anisotropy Maps

Microwave Foreground Frequency Spectra

There is a narrow window in frequency ranging from around 40 GHz to 150 GHz within which the CMB anisotropies dominate over other astrophysical foreground components.
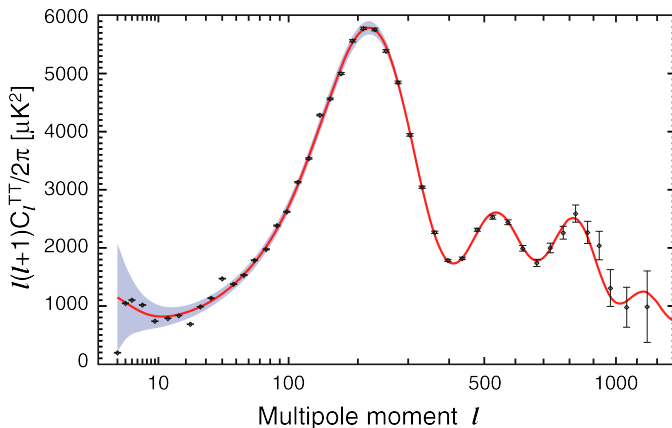
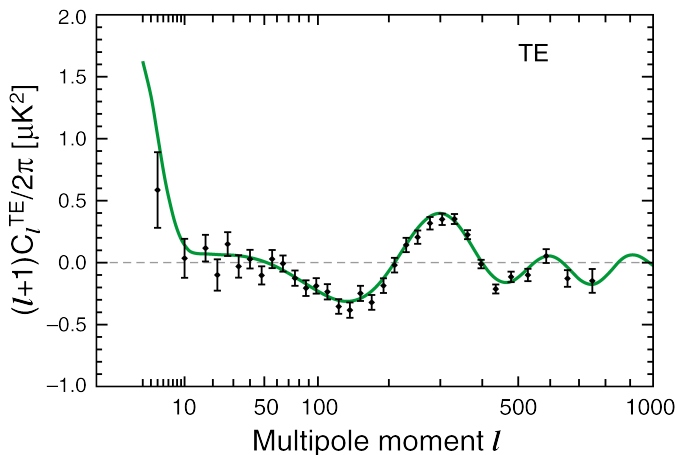# WMAP Temperature Anisotropy Maps

WMAP Polarization Anisotropy Maps

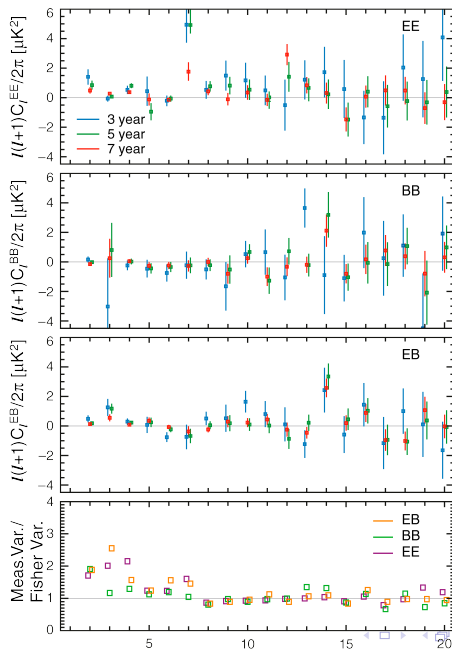# WMAP Temperature Power Spectrum

$$T(\hat{\Omega}) = \sum_{\ell=0}^{\infty} \sum_{m=-\ell}^{+\ell} a_{\ell m} Y_{\ell m}(\theta, \phi), \qquad c_{\ell} = \left\langle |a_{\ell m}|^2 \right\rangle$$
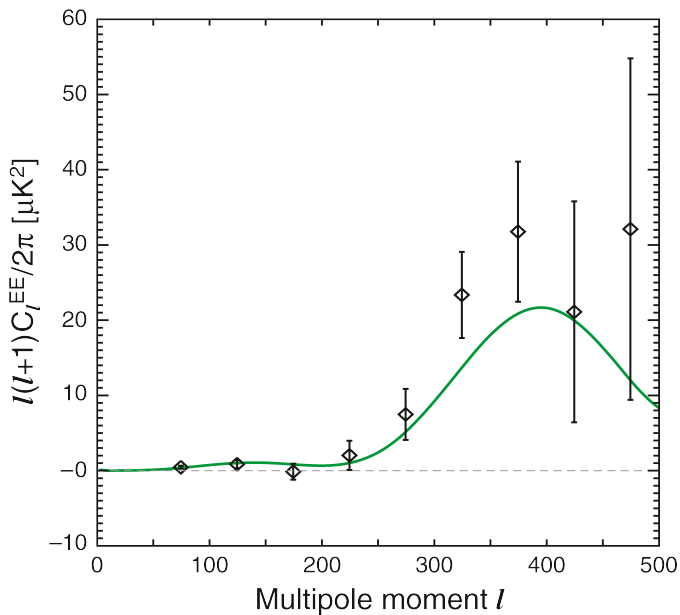
WMAP Temperature-E mode polarization cross power spectrum

WMAP polarization power spectrum (low-ℓ)

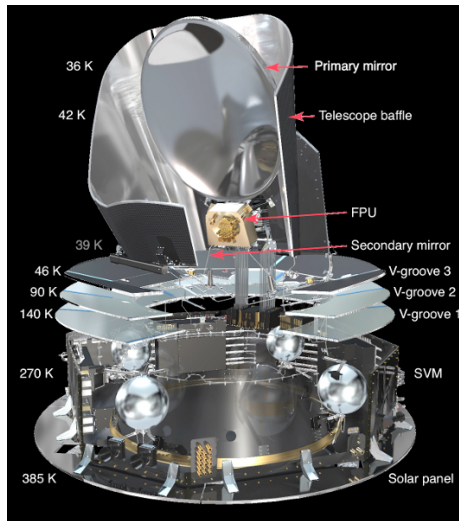# WMAP E-mode polarization power spectrum (high-ℓ)

WMAP 7-year best-fit cosmological parameters

WMAP Cosmological Parameters

Model: lcdm+sz+lens

Data: wmap7+bao+h0

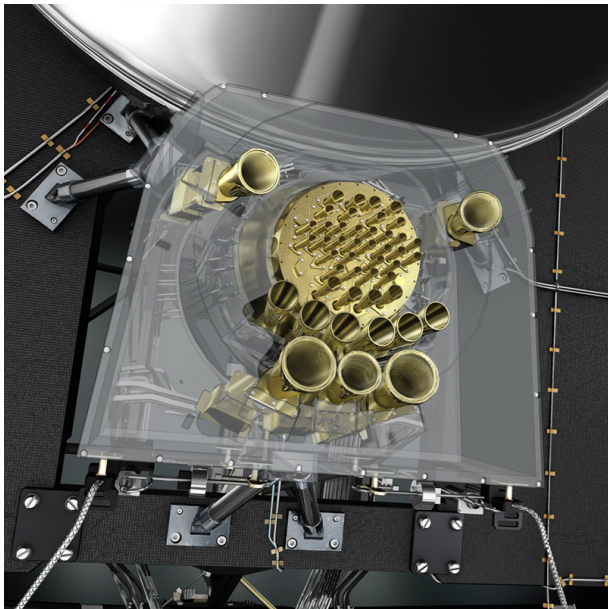|			
$10^2\Omega_b h^2$	2.260 ± 0.053	$1-n_s$	0.037 ± 0.012
$1-n_s$	$0.013 < 1-n_s < 0.061$ (95% CL)	$A_{\mathrm{BAO}}(z=0.35)$	0.468 ± 0.011
C_{220}	5762^{+38}_{-37}	$d_A(z_{\mathrm{eq}})$	14238^{+128}_{-129} Mpc
$d_A(z_*)$	14073^{+129}_{-130} Mpc	$\Delta_{\mathcal{R}}^2$	$(2.441^{+0.088}_{-0.092}) \times 10^{-9}$
h	$0.704^{+0.013}_{-0.014}$	H_0	$70.4^{+1.3}_{-1.4}$ km/s/Mpc
k_{eq}	0.00985 ± 0.00026	ℓ_{eq}	$138.6^{+2.6}_{-2.5}$
ℓ_*	302.40 ± 0.73	n_s	0.963 ± 0.012
Ω_b	0.0456 ± 0.0016	$\Omega_b h^2$	0.02260 ± 0.00053
Ω_c	0.227 ± 0.014	$\Omega_c h^2$	0.1123 ± 0.0035
Ω_Λ	$0.728^{+0.015}_{-0.016}$	Ω_m	$0.272^{+0.016}_{-0.015}$
$\Omega_m h^2$	0.1349 ± 0.0036	$r_{\mathrm{hor}}(z_{\mathrm{dec}})$	284.6 ± 1.9 Mpc
$r_s(z_d)$	152.7 ± 1.3 Mpc	$r_s(z_d)/D_v(z=0.2)$	$0.1904^{+0.0037}_{-0.0038}$
$r_s(z_d)/D_v(z=0.35)$	0.1143 ± 0.0020	$r_s(z_*)$	146.2 ± 1.1 Mpc
R	$1.7239^{+0.0100}_{-0.0099}$	σ_8	0.809 ± 0.024
A_{SZ}	$0.96^{+0.69}_{-0.96}$	t_0	13.75 ± 0.11 Gyr
τ	0.087 ± 0.014	θ_*	0.010389 ± 0.000025
θ_*	$0.5953 \pm 0.0014\,°$	t_*	377730^{+3205}_{-3200} yr
z_{dec}	1088.2 ± 1.1	z_d	1020.5 ± 1.3
z_{eq}	3232 ± 87	z_{reion}	10.4 ± 1.2
z_*	$1090.89^{+0.68}_{-0.69}$		

The Planck satellite

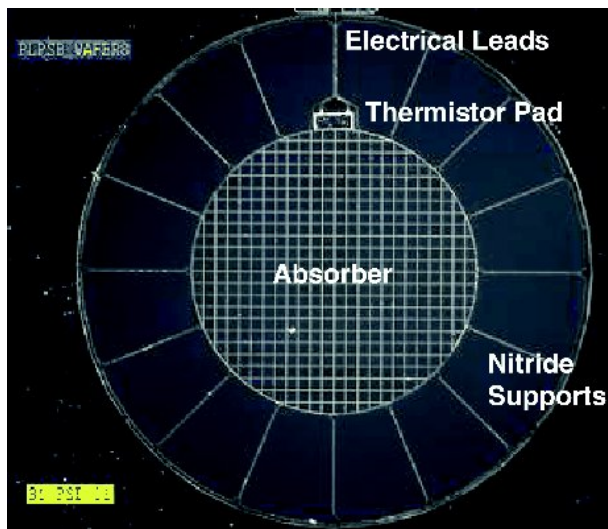(launched 13 May 2009, 30 months of data taken)
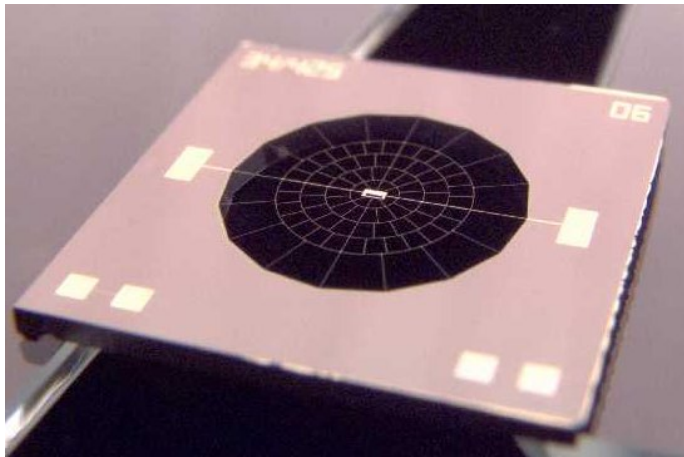
Planck collaboration

PLANCK Focal Plane

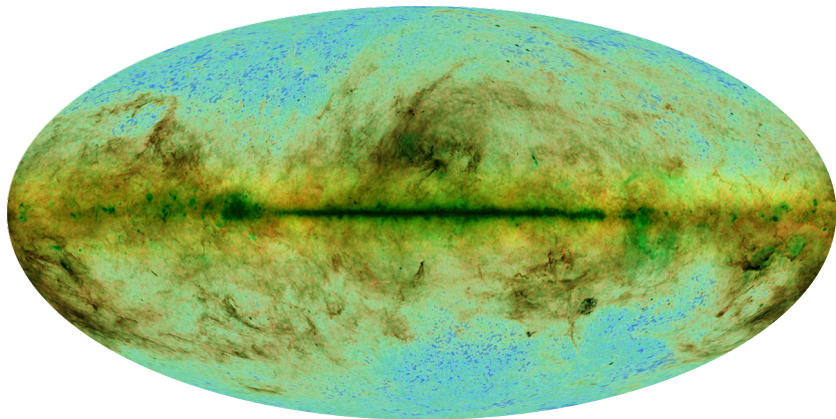# Polarization sensitive bolometers

Spider web bolometer

Planck Capabilities

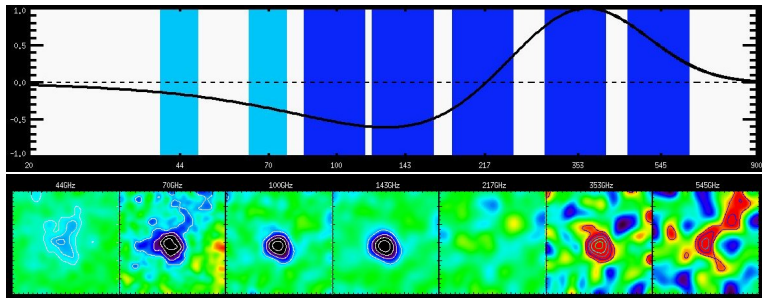| ν	n_{unpol}	n_{pol}	θ_{fwhm}	Temp (I) $\mu K \cdot$arcmin		Pol (Q,U) $\mu K \cdot$arcmin	
GHz			arcmin	RJ	CMB	RJ	CMB
30	4	4	32.7	198.5	203.2	280.7	287.4
44	6	6	27.9	228.0	239.6	322.4	338.9
70	12	12	13.0	186.5	211.2	263.7	298.7
100	8	8	9.9	23.9	31.3	33.9	44.2
143	11	8	7.2	11.9	20.1	19.7	33.3
217	12	8	4.9	9.4	28.5	16.3	49.4
353	12	8	4.7	7.6	107.0	13.2	185.3
545	3	0	4.7	6.8	1.1×10^3	—	—
857	3	0	4.4	2.9	8.3×10^4	—	—

PLANCK (30 month mission)

Planck sky

Planck frequency bands

Sunyaev-Zeldovich effect (clusters of galaxies

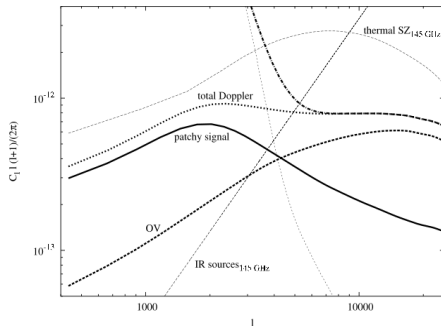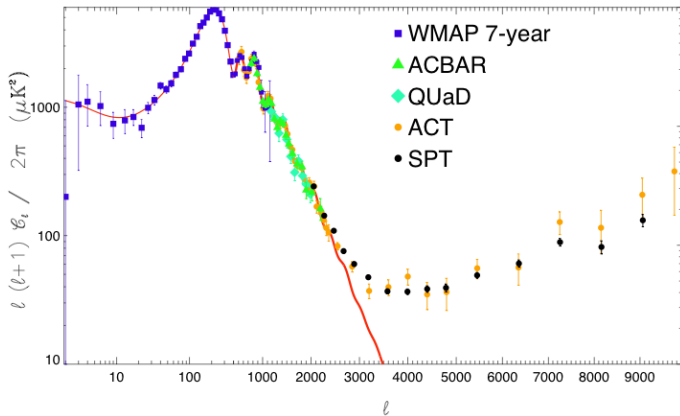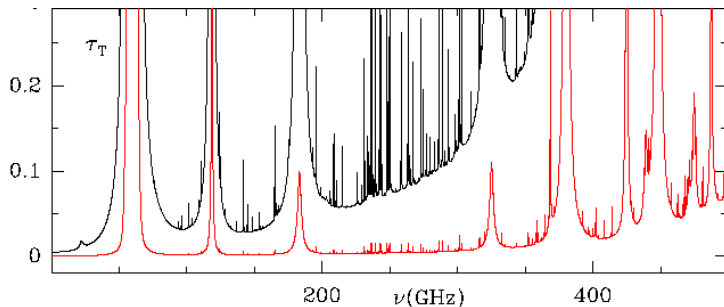# New effects take over at large ℓ

FIG. 8.— Different contributions to the total Doppler signal (kinetic SZ) in our extended patchy reionization Model C. The solid curve is the contribution to temperature anisotropies from the patchy regime alone at $z = 7 - 20$. The dashed curve gives the Doppler effect from density modulations at homogeneous ionization out to $z = 11$. The dotted curve sums up those contributions to the total Doppler signal. The total temperature fluctuations, cleaned of the thermal SZ and IR sources (shown at 145 GHz in the thin dashed lines), is given by the dot-dashed curve. These curves are smoothed versions of the power spectra generated from 50 maps.

Atmospheric interference. Calculated optical depth through the atmosphere for a good ground-based site like the South Pole or Dome-C in Winter (black) and at balloon altitude (red). Frequency bands for sub-orbital experiments must be carefully chosen to avoid the emission by molecular lines. Moreover, emission from oxygen lines is circularly polarized and care must be taken to avoid a significant polarized signal from the tails of these lines.

Observations from the ground (II)

Numerous CMB polarization experiments from the ground and balloons at various stages : QUaD, BICEP; BRAIN, CLOVER, EBEx, PAPPA, PolarBear, QUIET and Spider

- ▶ Far side lobes
- ▶ Scanning strategy (must scan at constant zenith angle)
- ▶ Polarization from interaction of Zeeman splitting by earth's magnetic field of oxgen lines. Atmospheric backscattering (very polarized) could be a serious problem. [See L. Pietranera et al., "Observing the CMB polarization through ice," MNRAS 346, 645 (2007)].
- ▶ Lack of stability and partial sky coverage

Photon shot noise

For a single mode :

$$\langle N \rangle = \Big(\exp(x) - 1 \Big)^{-1}, \qquad x = \left(\frac{h\nu}{k_B \, T_{CMB}} \right) = \left(\frac{\nu}{57 \; GHz} \right)$$

$$\langle N^2 \rangle = 2\langle N \rangle^2 + \langle N \rangle, \qquad \langle (\delta N)^2 \rangle = \langle N \rangle^2 + \langle N \rangle = N^2 + N$$
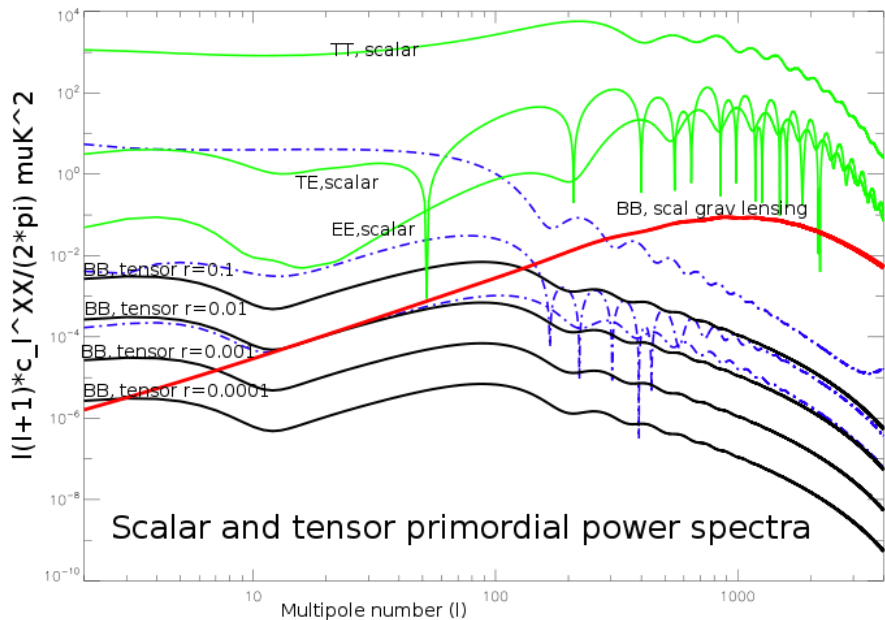
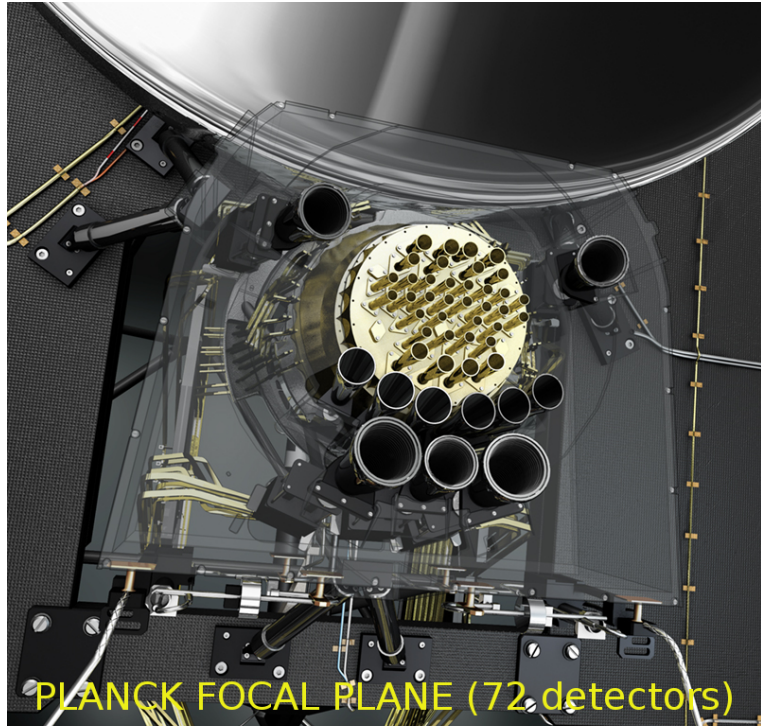$$\left(\frac{\delta N}{N} \right) = \sqrt{1 + N^{-1}}$$

For $x \gg 1$, pure Poissonian noise, almost. For $x \ll 1$, photon bunching (Hanbury Brown and Twiss) photons arrive roughly in bunches of N, these correlations augment noise relative to Poisson distribution.

Radio astronomers' formula (quantum corrected)

$$\left(\frac{\delta I}{I} \right) = \frac{1}{\sqrt{N_{det}}} \left(\frac{T_{sky} + \epsilon_{tel} \, T_{tel}}{T_{sky}} \right) \frac{1}{\sqrt{(\Delta\nu)t_{obs}}} \sqrt{e^{-1} + n_{occ}^{-1}}$$

$e = $ (quantum efficiency) = (prob. γ is absorbed), $\qquad T_{sky} \approx T_{CMB}$

$\epsilon_{tel} = $ (telescope emissivity)

Scalar and tensor primordial power spectra

Plot axes: $l(l+1)*c\_l^{}XX/(2*pi)$ muK^2 versus Multipole number (l)

Curve labels: TT, scalar; TE,scalar; EE,scalar; BB, scal grav lensing; BB, tensor r=0.1; BB, tensor r=0.01; BB, tensor r=0.001; BB, tensor r=0.0001
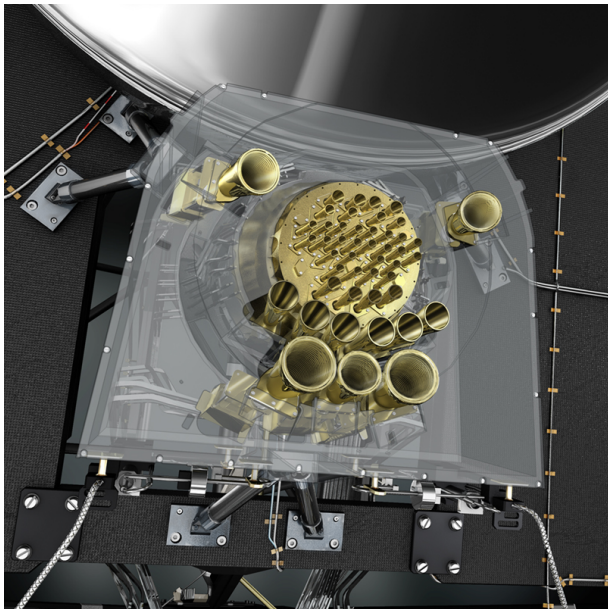
PLANCK FOCAL PLANE (72 detectors)

PLANCK Focal Plane

A Joint Analysis of BICEP2/Keck Array and Planck Data BICEP2/Keck and Planck Collaborations 2015 Submit

Planck intermediate results. XXX. The angular power spectrum of polarized dust emission at intermediate an

Planck 2015 results. I. Overview of products and results

Planck 2015 results. II. Low Frequency Instrument data processing

Planck 2015 results. III. LFI systematic uncertainties

Planck 2015 results. IV. LFI beams and window functions

Planck 2015 results. V. LFI calibration

Planck 2015 results. VI. LFI maps

Planck 2015 results. VII. High Frequency Instrument data processing: Time-ordered information and beam pr

Planck 2015 results. VIII. High Frequency Instrument data processing: Calibration and maps

Planck 2015 results. IX. Diffuse component separation: CMB maps

Planck 2015 results. X. Diffuse component separation: Foreground maps

Planck 2015 results. XI. CMB power spectra, likelihood, and consistency of cosmological parameters

Planck 2015 results. XII. Simulations Planck Collaboration

Planck 2015 results. XIII. Cosmological parameters

Planck 2015 results. XIV. Dark energy and modified gravity

Planck 2015 results. XV. Gravitational lensing

Planck 2015 results. XVI. Isotropy and statistics of the CMB

Planck 2015 results. XVII. Primordial non-Gaussianity

Planck 2015 results. XVIII. Background geometry and topology of the Universe

Planck 2015 results. XIX. Constraints on primordial magnetic fields

Planck 2015 results. XX. Constraints on inflation

Planck 2015 results. XXI. The integrated Sachs-Wolfe effect

Planck 2015 results. XXII. A map of the thermal Sunyaev-Zeldovich effect

Planck 2015 results. XXIII. Thermal Sunyaev-Zeldovich effect-cosmic infrared background correlation

Planck 2015 results. XXIV. Cosmology from Sunyaev-Zeldovich cluster counts

Planck 2015 results. XXV. Diffuse, low-frequency Galactic foregrounds

Planck 2015 results. XXVI. The Second Planck Catalogue of Compact Sources

Planck 2015 results. XXVII. The Second Planck Catalogue of Sunyaev-Zeldovich Sources

Planck 2015 results. XXVIII. The Planck Catalogue of Galactic Cold Clumps

http://www.cosmos.esa.int/web/planck/publications

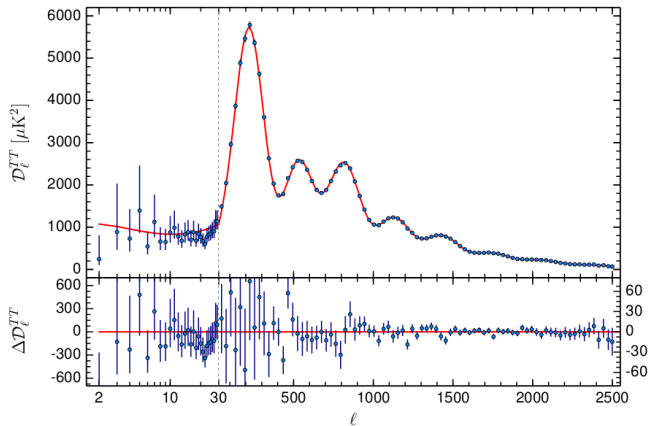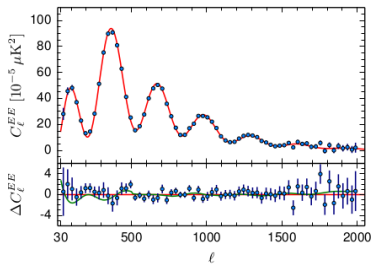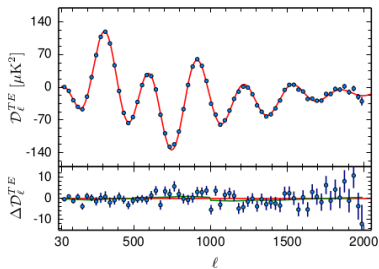# Temperature (TT) power spectrum with residuals

Fig. 1. The *Planck* 2015 temperature power spectrum. At multipoles $\ell \geq 30$ we show the maximum likelihood frequency averaged temperature spectrum computed from the `Plik` cross-half-mission likelihood with foreground and other nuisance parameters determined from the MCMC analysis of the base ΛCDM cosmology. In the multipole range $2 \leq \ell \leq 29$, we plot the power spectrum estimates from the `Commander` component-separation algorithm computed over 94% of the sky. The best-fit base ΛCDM theoretical spectrum fitted to the *Planck* TT+lowP likelihood is plotted in the upper panel. Residuals with respect to this model are shown in the lower panel. The error bars show $\pm 1\,\sigma$ uncertainties.

Polarization TE and EE spectra with residuals

The polarization PS reinforces the six-parameter orthodoxy

Fig. 6. Comparison of the base ΛCDM model parameter constraints from *Planck* temperature and polarization data.

Perturbations generated during inflation

$$\boxed{\hbar = c = 1, M_{pl}^{-2}} \qquad \delta\phi \approx H \qquad \frac{\delta\rho}{\rho} \approx H \cdot \delta t, \quad \delta t \approx \frac{\delta\phi}{\dot\phi}$$

$$H\dot\phi \approx V_{,\phi}, \quad \dot\phi \approx V_{,\phi}/H, \quad H^2 \approx \frac{1}{M_{pl}^2}V, \frac{\delta\rho}{\rho} \approx \frac{V^{3/2}[\phi(k)]}{M_{pl}^3 \ V_{,\phi}}$$

Scalar perturbations :
$$\boxed{\mathcal{P}_S^{1/2}(k) \approx O(1) \cdot \frac{V^{3/2}[\phi(k)]}{M_{pl}^3 \ V_{,\phi}[\phi(k)]}}.$$

Tensor perturbations :
$$\boxed{\mathcal{P}_T^{1/2}(k) \approx O(1) \cdot \frac{H}{M_{pl}} \approx O(1) \cdot \frac{V^{1/2}}{M_{pl}^2}}$$

$\phi(k) \equiv$ value of ϕ at horizon crossing of the mode k

Reconstruction of the inflationary potential : the tensors measure the height of the potential, the scalars the slope.

Fig. 12. Marginalized joint 68 % and 95 % CL regions for n_s and $r_{0.002}$ from *Planck* in combination with other data sets, compared to the theoretical predictions of selected inflationary models.

What is the primordial power spectrum ?

▶ For lack of a fundamental theory, expand in powers of $\ln(k)$

$$
\begin{aligned}
\ln\left(\mathcal{P}(\ln k)\right) &= \mathcal{P}_0 \left(\ \ln(k/k_{piv})\right)^0 + \mathcal{P}_1 \left(\ \ln(k/k_{piv})\right)^1 + \mathcal{P}_2 \left(\ \ln(k/k_{piv})\right)^2 + \ldots \\
\mathcal{P}(k) &= A(k/k_{piv})^{(n_s-1)} \\
&\quad \text{or} \\
\mathcal{P}(k) &= A(k/k_{piv})^{(n_s-1)+\alpha \ln(k/k_{piv})+\ldots}
\end{aligned}
$$

▶ *Planck* seems to be telling us that the first two terms suffice, and using just the first term can be ruled out at a respectable statistical significance. $n_S \neq 1$ implies exact scale invariance needs to be downgraded to an approximate symmetry. No statistically significant evidence for running of the spectral index.

Penalized likelihood

$$\mathbf{f}^{\mathrm{T}} \mathbf{R}(\lambda, \alpha) \mathbf{f} \equiv \lambda \int \mathrm{d}\kappa \left(\frac{\partial^2 f(\kappa)}{\partial \kappa^2} \right)^2$$

$$+ \alpha \int_{-\infty}^{\kappa_{\min}} \mathrm{d}\kappa \, f^2(\kappa) + \alpha \int_{\kappa_{\max}}^{+\infty} \mathrm{d}\kappa \, f^2(\kappa).$$

$$\kappa = \ln(k), \quad f(\kappa) = A_S \, k^{n_S} [1 + f(k)]$$

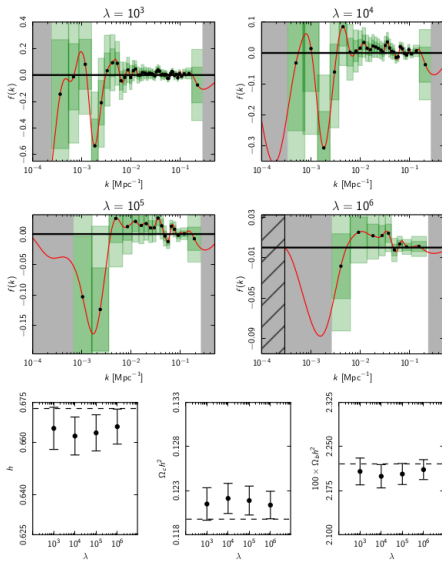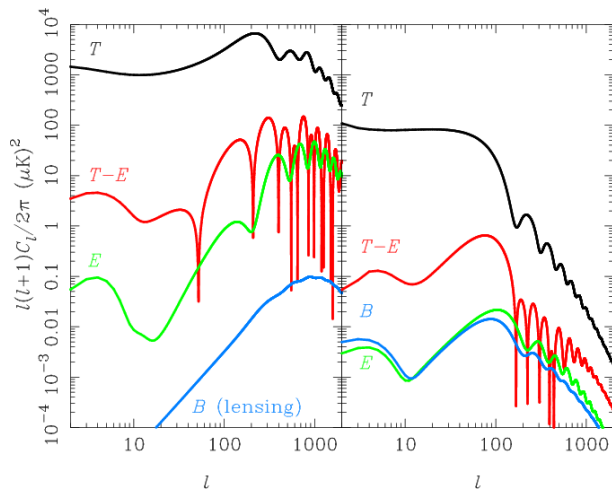**Fig. 21.** *Planck* TT likelihood primordial power spectrum (PPS)

Fig. 22. *Planck* TT,TE,EE+lowTEB likelihood primordial power spectrum reconstruction results. *Top four panels*:

Constraining tensor modes

Detecting tensor modes with the CMB TT power spectrum

r=0.24

Taken from : Challinor, astro-ph/1210.6008

BICEP2 claim on Planck-like plot

Fig. 54. Marginalized joint 68 % and 95 % CL regions for n_s and $r_{0.002}$ from *Planck* alone and in combination with its cross-correlation with BICEP2/Keck Array and/or BAO data compared with the theoretical predictions of selected inflationary models.

Constraining tensors with B modes :
A clean probe

E and B Mode Polarization

E mode   B mode

$$\mathbf{Y}^{(E)}_{\ell m, ab} = \sqrt{\frac{2}{(\ell-1)\ell(\ell+1)(\ell+2)}} \left[\nabla_a \nabla_b - \frac{1}{2}\delta_{ab}\nabla^2 \right] Y_{\ell m}(\hat{\Omega})$$

$$\mathbf{Y}^{(B)}_{\ell m, ab} = \sqrt{\frac{2}{(\ell-1)\ell(\ell+1)(\ell+2)}} \frac{1}{2} \left[\epsilon_{ac}\nabla_c\nabla_b + \nabla_a\epsilon_{bc}\nabla_c \right] Y_{\ell m}(\hat{\Omega})$$

Projection of « scalars, » « vectors » and « tensors » onto the celestial sphere

Under projection onto the celestial sphere :

$$(scalar)_3 \rightarrow (scalar)_2,$$

$$(vector)_3 \rightarrow (scalar)_2 + (vector)_2,$$

$$(tensor)_3 \rightarrow (scalar)_2 + (vector)_2.$$

There is no $(tensor)_2$ component. The E mode polarization is scalar ; the B mode is vector.

It follows that at linear order the scalar modes cannot generate any B mode polarization.

Note crucial role of linearity assumption.

Inflationary Prediction for Scalar & Tensor Anisotropies

The Reionization Bump

It turns out that

$$P \propto (1 - \tau) d^2_{lastscatter} \frac{\partial^2 T}{\partial x^2}$$

is small compared to

$$P \propto \tau d^2_{reion} \frac{\partial^2 T}{\partial x^2}$$

even when τ is small.

Breaking news 22 March 2014

BICEP2 summary plot :

"Smoking gun" of gravitational waves from inflation?

30   44   70   100   143   217   353   545   857

30–353 GHz: δT [μK$_{CMB}$]; 545 and 857 GHz: surface brightness [kJy/sr]

From Planck Collaboration : Dust polarization at high latitudes
(astro-ph/1409.3738)
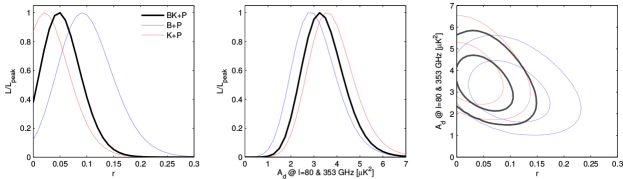
r<0.12 at 95 % now from B modes

FIG. 6. Likelihood results from a basic lensed-ΛCDM+r+dust model, fitting BB auto- and cross-spectra taken between maps at 150 GHz, 217, and 353 GHz. The 217 and 353 GHz maps come from *Planck*. The primary results (heavy black) use the 150 GHz combined maps from BICEP2/*Keck*. Alternate curves (light blue and red) show how the results vary when the BICEP2 and *Keck Array* only maps are used. In all cases a Gaussian prior is placed on the dust frequency spectrum parameter $\beta_{\rm d} = 1.59 \pm 0.11$. In the right panel the two dimensional contours enclose 68% and 95% of the total likelihood.

LiteBIRD Instrument

- Mission module benefits from heritages of other missions (e.g. ASTRO-H) and ground-based experiments (e.g. POLARBEAR).
- Bus module based on high TRL components

Multi-chroic focal plane detectors

Lenslet

TES   MKID

Cryogenics
- JT/ST and ADR (ASTRO-H heritage)

Line of sight
FOV 10 x 20 deg.
0.1rpm spin rate
30 deg.

Mission module

slip ring

Solar array paddle

Bus module

HGA: X band data transfer to the ground

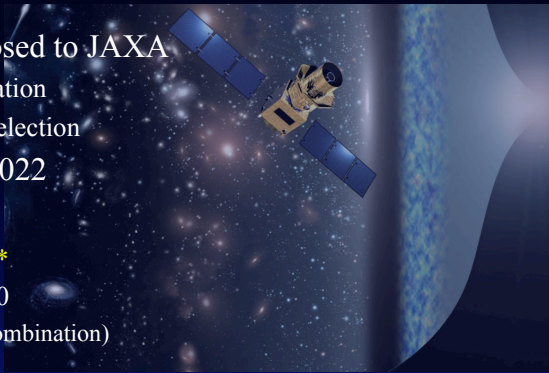Continuously-rotating half wave plate (HWP)

Incident radiation

Rotating HWP at aperture
4 K

Secondary mirror
4 K

Focal plane
100 mK

Primary mirror 4 K

400 mm

Mirrors at 4K

LiteBIRD Overview

Lite (Light) Satellite for the Studies of B-mode Polarization and Inflation from Cosmic Background Radiation Detection

- CMB B-mode satellite proposed to JAXA
  - Also to NASA for US participation
  - Both proposals passed initial selection
- Proposed launch year: JFY 2022
- Mission Requirements
  - Total uncertainty on r < 0.001*
  - Multipole coverage: $2 \leq \ell \leq 200$
    - Each bump (reionization, recombination) with >5 sigma if $r > 0.01$
- Orbit: L2
- Observing time: 3 years

*Our current studies yield $\sigma(r) = 2 \times 10^{-4}$ (for r=0) for 3 year observation

15 frequency bands

Polarization sensitivity

2.4 μKarcmin

(3 year operation, including margin)